JMEPEG (2000) 9:541-551

Microstructural and Mechanical Investigation of Aluminum Tailor-Welded Blanks

P.A. Friedman and G.T. Kridli

(Submitted 22 March 2000)

The push to manufacture lighter-weight vehicles has forced the auto industry to look to alternative materials than steel for vehicle body structures. Aluminum is one such material that can greatly decrease the weight of vehicle body structures and is also consistent with existing manufacturing processes. As in steel structures, cost and weight can be saved in aluminum structures with the use of tailored blanks. These blanks consist of two or more sheets of dissimilar thicknesses and/or properties joined together through some type of welding process. This enables the design engineer to "tailor" the blank to meet the exact needs of a specific part. Cost savings can be gained by the elimination of reinforcement parts and the stamping dies used to manufacture them. Weight savings can be attained based on the fact that one thicker piece is more efficient than a welded structure and therefore can allow for down-gauging of parts.

Although tailor-welded blanks (twbs) offer both potential weight and cost benefits, the continuous weld-line and thickness differential in twbs can often result in difficulty in stamping. This problem is more severe in aluminum because of its limited formability as compared with typical drawing-quality steels. Additionally, welding of steel twbs tends to increase the strength of the weld material, which helps prevent failure in the weld during forming. Aluminum twbs do not experience this increase in strength and therefore may have a greater tendency to fail in the weld. In this study, several aspects of twbs manufactured from 6111-T4, 5754-O, and 5182-O aluminum alloys were analyzed and compared with those of a more conventional steel twb. The effect of gauge mismatch on the formability of these blanks is discussed as well as the overall potential of these blanks for automotive applications.

Keywords aluminum, mechanical-properties, microscopy, stamping, welding

1. Introduction

Ongoing pressure to reduce vehicle weight has forced automotive manufacturers to look to alternative materials than steel for vehicle body construction. One material that is consistent with existing manufacturing processes and has attractive qualities such as low density, good mechanical properties, and high corrosion resistance is aluminum. It has been estimated that replacing steel with aluminum in body-in-white and closures can result in weight savings as high as 55%. However, the reduced formability and weldability of aluminum as compared with steel presents several technical challenges.

The use of tailor-welded blanks (twbs) in the construction of vehicle body structures and closures has increased dramatically in the last few years.[1] By connecting two sheets of dissimilar thicknesses and/or properties to create a twb, it is possible to manufacture parts with variable properties. This can result in the elimination of reinforcement parts, which, in turn, can lead to savings in weight and cost.[2] Additionally, these blanks are often stiffer than conventional reinforced structures, thus making it possible to down-gauge these parts and obtain further weight savings. With increasing aluminum content in vehicles, the natural step in the effort to produce lighter-weight vehicles will be to incorporate tailor-welded technology in aluminum structures.

The gauge differential intrinsic to twb technology may result in strain localization during stamping. This problem may potentially be more severe in aluminum because of its limited formability as compared with typical drawing-quality steels. The objective of this paper is to develop an understanding of aluminum twbs and how they differ from steel twbs. First, the effect of alloy is considered by investigating twbs of two different alloy series (AA5xxx and AA6xxx) manufactured from the same gauge material and comparing them with a steel twb. Welded blanks manufactured from same-gauge sheet are used to isolate problems associated with the weld from problems that may be associated with using dissimilar gauge materials. A twb manufactured from dissimilar gauge from a slightly different alloy (AA5182) is then studied to determine the effect of gauge mismatch on the feasibility of aluminum twbs. Mechanical testing and optical microscopy are used to characterize the material, and formability testing is used to determine how the material will perform in production stamping.

2. Material for Study

Sheet alloys from two different families have been used for automotive applications. The heat-treatable 6111-T4 is used for exterior body panels, such as hoods, fenders, and decklids because of its relatively high dent resistance and good strength. Heat treatable alloys are often used for this type of application because they do not attain their final strength until after the

P.A. Friedman, Ford Research Laboratory, Dearborn, MI 48121-2053; and **G.T. Kridli**, Industrial and Manufacturing Systems Engineering, University of Michigan-Dearborn, Dearborn, MI 48128-1491. Contact e-mail:pfriedma@ford.com.

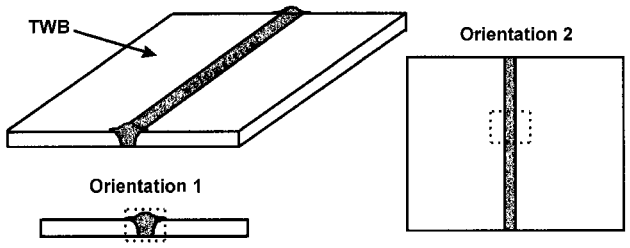

Fig. 1 Weld orientations for optical microscopy

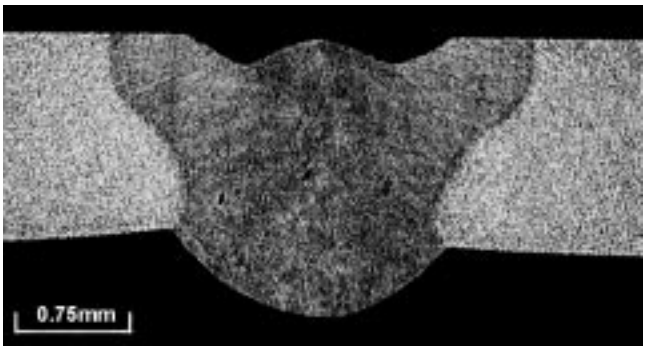

Fig. 2 Micrograph of the weld joint in AA5754 in orientation 1

Table 1 Summary of twbs selected for this study

Alloy	Gauge, mm	Gauge, mm	Welding technology
5754-O	1.6	1.6	ND: YAG
6111-T4	1.0	1.0	ND: YAG
5182-O	0.84	1.55	ND: YAG
Low-carbon steel	0.7	0.7	CO_2

paint-bake cycle during which they precipitation harden, thus minimizing forming problems such as springback. Al-Mg alloys, such as AA5754-O and AA5182-O, have been used in structural body applications because of their relatively high ductility, which is needed for stamping the thicker gauge structural components. The twbs manufactured from these alloys are described in Table 1.

3. Alloy Considerations

3.1 Microscopy

Material samples from the welded sheets of the same-gauge AA5754 and AA6111 twbs were removed from the center of the sheets and mounted for metallographic study. Samples were prepared in two different orientations, as shown in Fig. 1, and then mechanically ground and polished for optical microscopy.

The AA5754 alloy was electrochemically etched with a fluorboric acid solution to reveal the microstructure. A relatively low magnification picture of the weld profile in orientation 1 is shown in Fig. 2. The weld can be clearly identified in the middle of the micrograph by the apparent difference in color.

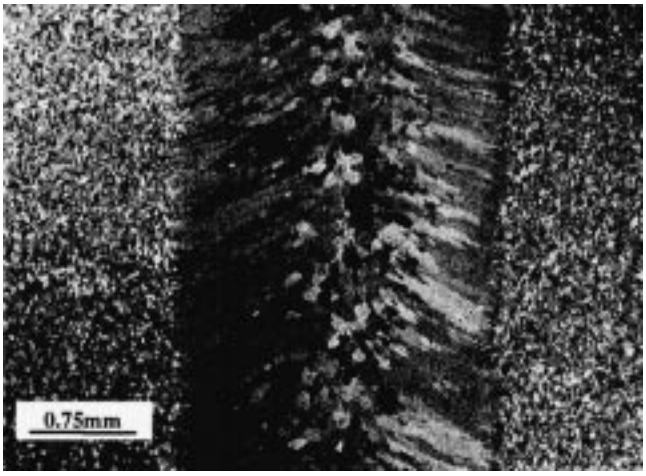

Fig. 3 Micrograph of the weld in the AA5754 twb in orientation 2 depicting the weld profile and the flow of material during solidification

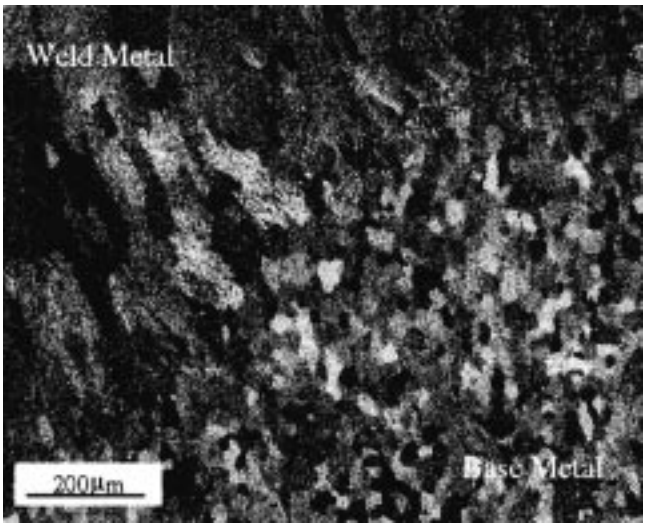

Fig. 4 Higher magnification micrograph of AA5754 in orientation 1 depicting the transition zone between the weld and base materials

This is a result of preferential etching in and out of the weld area. The funnel-type shape of the weld is typical of aluminum twbs. However, the notches on the welding side of the blank (top side) will produce stress-intensity factors during forming that may result in premature failure of the sheet in forming trials. This effect is somewhat offset by the large degree of drop-through in the weld (hemispherical protrusion on the bottom side of the weld).

The flow of the weld material during solidification is shown in Fig. 3, which is a micrograph of the top side of the weld (orientation 2). Here the flow pattern of material in the weld region can be deciphered. Typical of aluminum welds, the middle of the weld contains relatively equiaxed grains, whereas the sides of the weld contain columnar grains. These columnar grains are formed from epitaxial growth of the base material into the center of the weld. Note that the elongated grains are not perpendicular to the base material, but rather at an angle

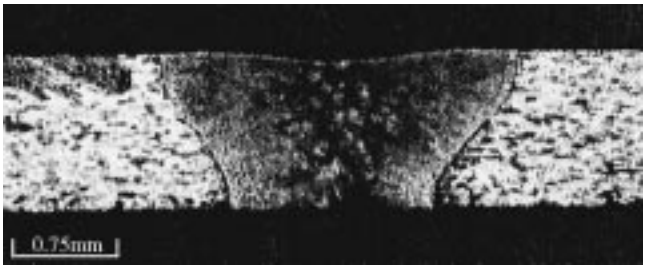

Fig. 5 Micrograph of the weld joint in AA6111 in orientation 1

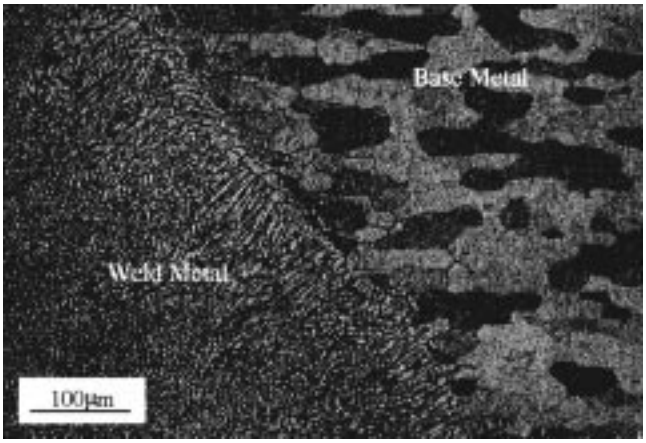

Fig. 6 Higher magnification micrograph of AA6111 in orientation 1 depicting the transition zone between the weld and base materials

due to the laser's movement during the welding process. This angle tends to widen with increases in welding speed. Whether this inhomogeneity of the weld material will have a deleterious effect on the blank during stamping is an issue that needs further investigation.

A higher magnification picture of the welded sheet is shown in Fig. 4 depicting the transition zone between the weld and base materials. The differences between the base wrought material and the resolidified weld area are readily apparent. The base material appears to have a typical wrought aluminum microstructure with a relatively fine grain size. On the other hand, the welded material seems to have experienced a complete remelt and is in the as-cast condition. Based on the relatively small cell size in the weld material, it may be inferred that the material underwent a very rapid solidification after the remelt. The grain sizes in both the base and weld areas were measured by the linear intercept method as 19.56 and 64.3 μm, respectively. It was assumed from this large grain-size disparity that there would be a significant difference in strength between the weld and the base material. However, this difference was not found during mechanical testing and is further examined in Section 6.

The AA6111 samples were etched with a light Keller's solution to reveal the microstructure. The weld profile in orientation 1 is shown in Fig. 5. Similar to the AA5754 alloy, the weld profile is somewhat funnel shaped. However, unlike the 5754 sample, this blank has a relatively sharp notch on the bottom side of the weld. This notch, most likely due to *suck back* during welding, appears to be the beginning of a crack, possibly formed during solidification.

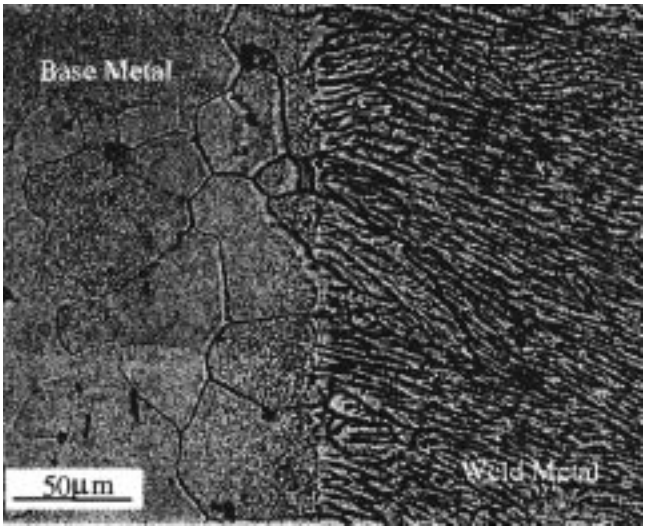

Fig. 7 Higher magnification micrograph of AA6111 in orientation 2 depicting the transition zone between the weld and base materials

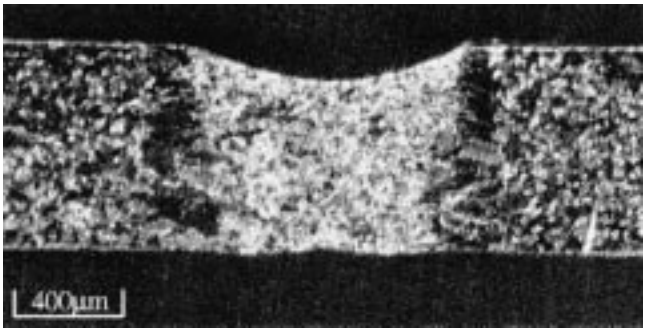

Fig. 8 Micrograph of the steel twb in orientation 1

The transition zone for the AA6111 material is shown in Fig. 6 in orientation 1. Similar to the AA5754 material, there is a very fine transition between the weld and the base materials. This can be seen in more detail in Fig. 7 in orientation 2, where the dividing line between material that had melted to material that was unaffected by the welding is apparent. Again, it appears that the weld material has a very small cell size, indicating a relatively fast solidification time.

The effect of the remelt on the mechanical properties of the material was predicted to be relatively large for this alloy because of the T4 temper the material was in prior to welding. The weld material is resolidified and therefore loses any age hardening it may have undergone since the material was originally processed. This loss of strength in the weld area was confirmed by hardness measurements as shown below and is consistent with the work of Stasik and Wagoner.[3]

In Fig. 8, the micrograph of the steel twb is shown in orientation 1. A few interesting things can be noted from this micrograph. The weld appears to be more rectangular and does not display the funnel-like profile of the aluminum welds. Furthermore, the weld area contains a very gradual notch and

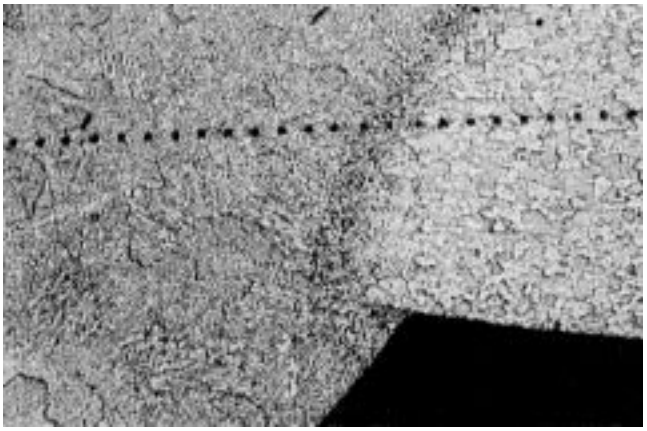

Fig. 9 Examples of indentations made from the UMIS 2000 nanoindenter

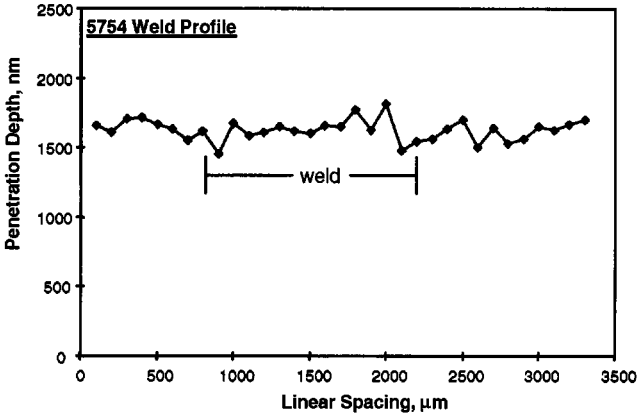

Fig. 10 Penetration depth profile for both the base and weld materials as determined by the nanoindentions on the AA5754 twb

Table 2 Results of tensile testing and subsequent optical microscopy

Specimen	Overall strain, %	Strain in the weld, %	β, (Ratio of strain in weld to strain in gauge length)	Fracture site
AA5754	8.1	20.8	2.57	weld
AA6111	0.4	18.4	46.0	weld
Steel	38.6	18.0	0.47	base

subsequently a decreased gauge in the weld area. While this decreased gauge acts as a stress riser, tensile test results show that the strain does not tend to localize in this region during deformation (Table 2). Similar to the aluminum samples, the drawing of material into the weld during resolidification is evident, denoted by columnar grains in the area between the weld and base materials.

3.2 Nanoindentation and Hardness Measurements

The UMIS-2000 (Wilson Instruments, Canton, MA) nanoindenter was used to measure hardness inside the base and weld areas. The indenter, equipped with a 5 μm hemispherical diamond tip, measures the response at each point by incrementally applying load in 20 steps up to the maximum. Between each

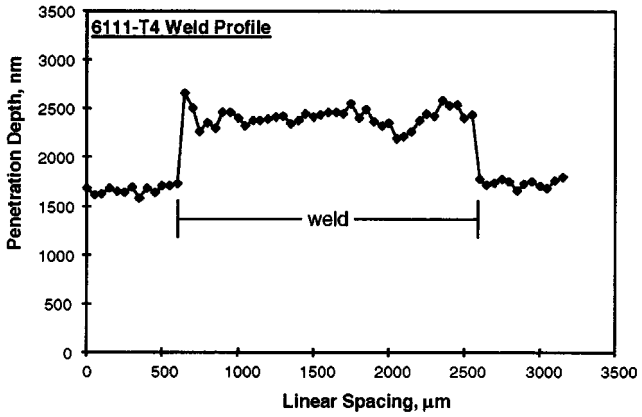

Fig. 11 Penetration depth profile for both the base and weld materials as determined by the nanoindentions on the AA6111 twb

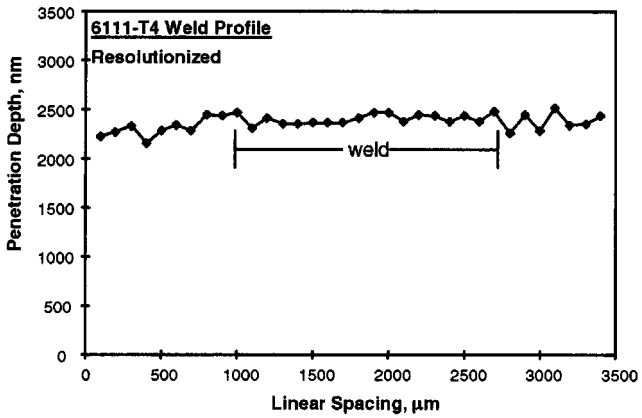

Fig. 12 Penetration depth profile for both the base and weld materials as determined by the nanoindentions on the AA6111 twb after resolutionizing

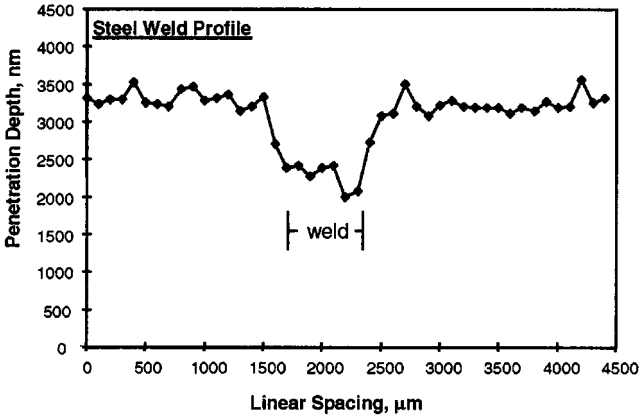

Fig. 13 Penetration depth profile for both the base and weld materials as determined by the nanoindentions on the steel twb

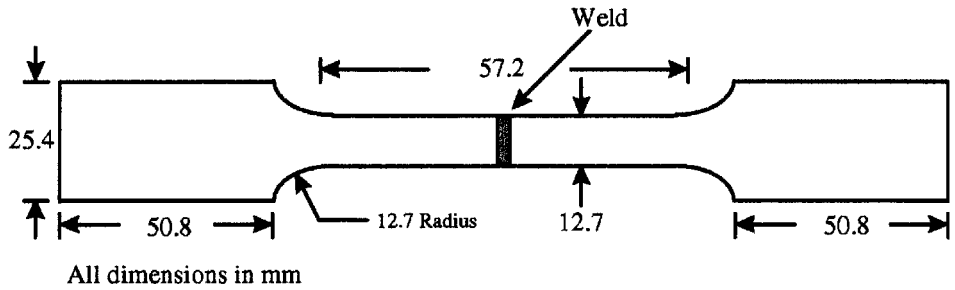

Fig. 14 Schematic of the tensile specimen depicting the orientation of the weld line with the tensile axis

Fig. 16 Tensile fracture of AA6111 twb

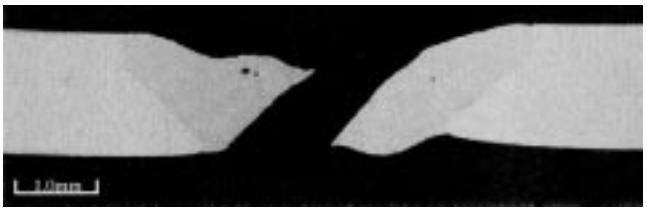

Fig. 15 Tensile fracture of AA5754 twb

load step, the device decreases the load by half to measure the elastic recovery. This 20-step loading schedule is performed at each place a measurement is taken. The hardness and elastic modulus can then be determined as a function of penetration depth. In this study, the penetration depth at full load was used as an indicator of the relative strength of the material. These measurements were taken across the material in orientation 1 to determine the relative strengths of the base and weld materials. Examples of these indents are shown in Fig. 9.

For the AA5754 welded blank, a load of 50 mN was used to probe the hardness of the material in the weld and base materials. The penetration depth profile at locations across the material, crossing through the weld area, is shown in Fig. 10. It appears from this plot, that there is only a slight increase in penetration depth in the weld area. It is believed that the loss of strength and hardness that is expected due to the grain size differential in the weld and base materials is somewhat offset from a strong residual stress field and a small cell spacing in the weld area.

Contrary to this, the hardness profile for the 6111 alloy, shown in Fig. 11, displays a pronounced difference in hardness between the weld and base areas. This is seen in the increased penetration depth in the weld area. This loss of strength is a result of removing the age hardening (T4 temper) in the weld material during the remelt and solidification of welding. To confirm this theory, a piece from the 6111 twb was resolutionized at 545 °C for 5 min to equalize the thermal treatments of the base and weld materials. The resulting penetration profile, shown in Fig. 12, confirms that the decrease in weld strength is due to the elimination of the T4 temper in the weld area. As a comparison to these aluminum twbs, nanoindent data were collected for the steel sample at a load of 100 mN. In Fig. 13, the penetration depth profile for the steel material is shown. The lower penetration depths in the weld area are consistent with the tensile results (shown below), which indicate the material is stronger in the weld than in the base.

Microhardness measurements were made with a Vickers hardness tester to confirm the hardness measurements determined from the nanoindenter. As expected, the overall trends in hardness inside and outside of the weld material are consistent.

3.3 Tensile Testing

Tensile coupons were machined from the welded sheet material with the weld oriented in the middle of the gauge section perpendicular to the tensile axis (Fig. 14). Multiple tensile specimens were deformed on an MTS machine at a constant crosshead speed of 3 mm/min until fracture. A 50.8 mm extensometer was attached to the specimens to track overall strain in the gauge region. After testing, material was extracted from the fracture zone and mounted for optical microscopy.

Strain in the weld area was approximated by measuring the weld zone before and after tensile testing and comparing this with the overall tensile strain in the gauge length. The ratio of these two values, defined as

$$\beta = \frac{\varepsilon_w}{\varepsilon_o} \qquad \text{(Eq 1)}$$

where ε_w is the strain in the weld and ε_o is the overall tensile strain, can be used as a simple estimate of a twb's quality and strength. This variable is an indicator of the propensity of a twb to experience strain localization in the weld and fail during forming.

Tensile tests on the AA5754 material resulted in fracture in the weld zone for all tests. The average strain to failure in these samples was 8.1%. However, measurements of the weld before and after deformation indicated that the average strain in the weld was 20.8%. This localization can be seen in Fig. 15 where the fracture in the weld is shown. The average β value for these blanks was 2.57, indicating that strain localized in the weld area.

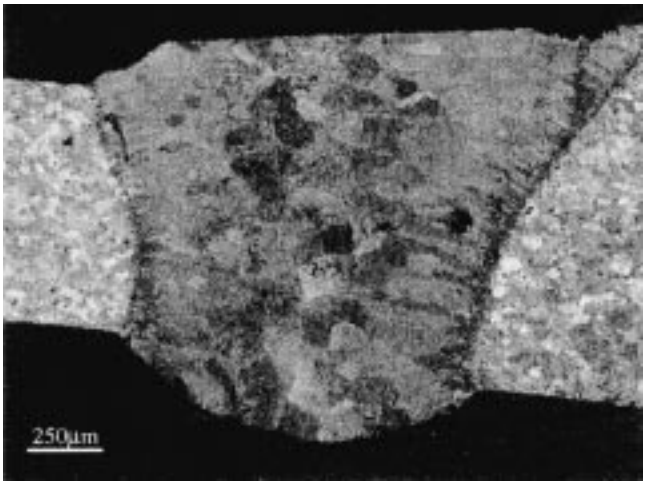

Fig. 17 Micrograph of the weld joint in AA5182 in orientation 1 depicting the attachment of the two dissimilar gauges

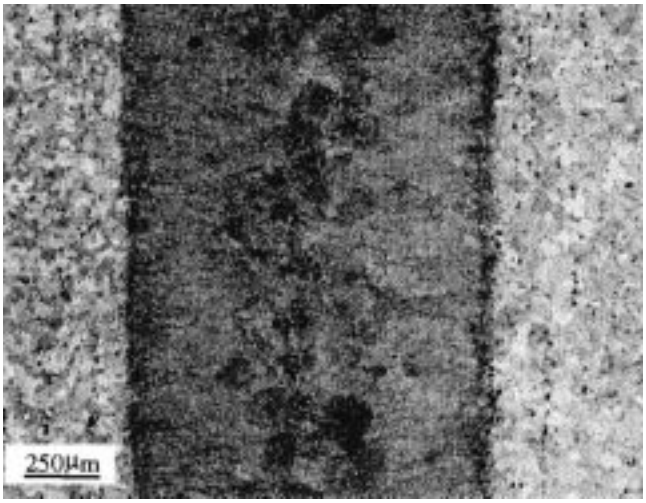

Fig. 18 Micrograph of the weld joint in AA5182 in orientation 2

Table 3 Results of tensile testing and subsequent optical microscopy

Specimen	Overall strain, %	Strain in the weld, %	β	Fracture site
AA5182	12.8(a)	7.55	0.59	base
AA5754	8.1	20.8	2.57	weld

(a) Strain to failure on thin side of weld was 24.4%. Uniform strain across the gauge length was 12.8%.

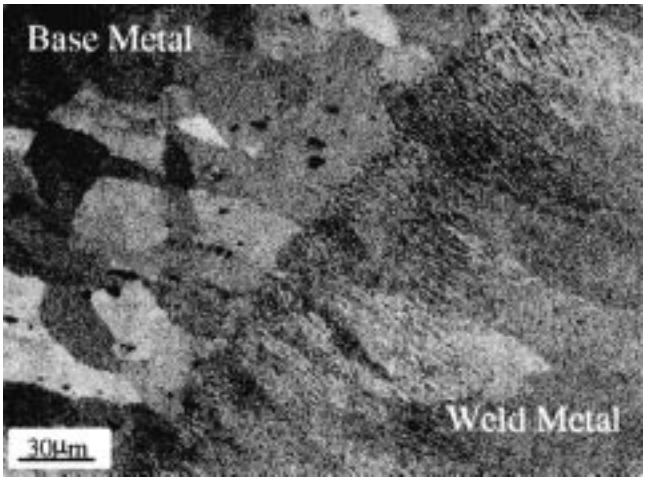

Fig. 19 Higher magnification micrograph in orientation 1 of the transition zone in the AA5182 weld

Similar to the AA5754 material, the AA6111 material failed in the weld during all tensile tests. However, the material failed after only an average strain of 0.4%, most likely due to the combined effect of the weaker material in the weld and the effect of the notch as a stress intensifier. The fracture zone is shown in Fig. 16. Measurements of the weld before and after deformation indicated that the weld experienced a strain of 18.4%. This indicates that the weld material retained its ductility after the welding process and that the failure is due to either the lower strength in the weld or the reduced cross-sectional area. This intense localization of strain is seen in the relatively high β value of 46.

Conversely, the steel twbs did not fail in the weld area, but rather at random locations across the gauge section. As shown in Table 2, the strain in the weld was significantly lower than the overall strain in the gauge length. This resulted in a relatively low β value of 0.47, which implies the weld material in the steel twb is stronger than the base material, unlike either of the aluminum twbs. A summary of the tensile test results on all three twbs is shown in Table 2.

4. Dissimilar Gauge Effects

While the relative strength of the weld to the base material is an important aspect of twb technology, another potential issue is the effect of dissimilar gauge on the formability of these blanks. This problem is more severe in aluminum because the weld is typically not stronger than the base material, as often is the case with steel. In this next series of experiments, a twb manufactured from two gauges of AA5182 material was studied and compared with the earlier results on the same-gauge AA5754 material. While these two twbs were manufactured from slightly different alloys, the major difference between same-gauge and dissimilar gauge twbs is demonstrated.

4.1 Microscopy

Samples from the weld line in the AA5182 were prepared in an identical method as in the AA5754. A low-magnification micrograph of the weld in orientation 1 is shown in Fig. 17. The weld is the attachment point of material of two different gauges and is characterized by a smooth top side with a protrusion (drop-through) on the bottom side.

The increased cross-sectional area in the dissimilar gauge AA5182 twb is critical in the prevention of premature fracture

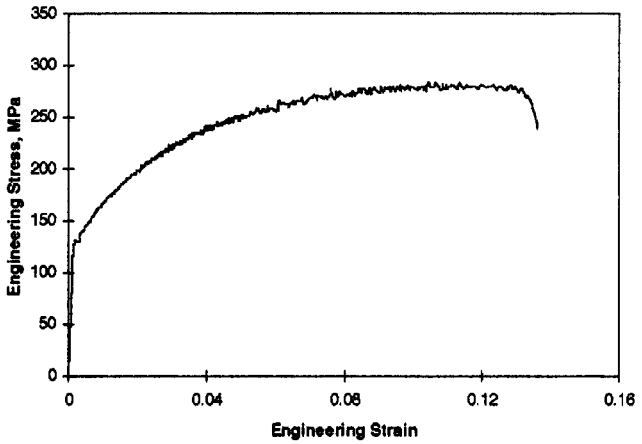

Fig. 20 Stress-strain curve determined from tensile tests on AA5182 twb. Strain was measured with a 50.8 mm extensometer placed equally across the thin and thick sides of the gauge length (Fig. 14)

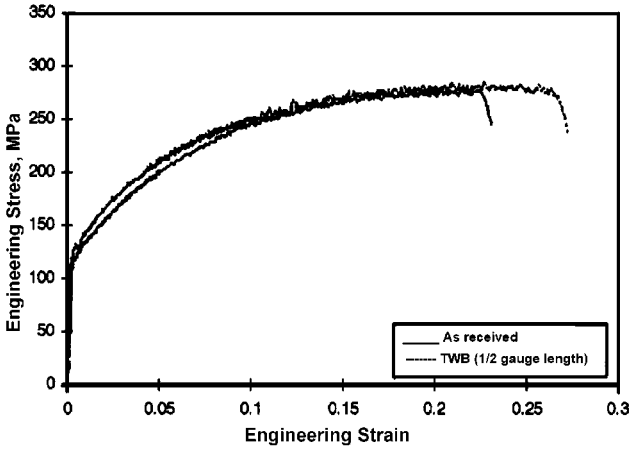

Fig. 21 Stress-strain plots of both material without the weld and recalculated data from Fig. 20 based on half of the actual gauge length

in the weld zone. The weld profile in the AA5754 has a slightly reduced cross section and therefore is not as resistant to strain localization. This is most likely due to the fact that the AA5754 material consists of welded blanks of identical gauge. The step in gauge in this current material allows for a smooth transition from one gauge material to the other without producing a gauge reduction in the weld zone (Section 6).

In Fig. 18, the weld is shown in orientation 2. Similar to the AA5754 blanks, the weld consists of larger grains in the center of the weld with elongated grains closer to the interface of the base and weld zones. The elongated grains in this AA5182 alloy appear to be nearly perpendicular to the base-weld interface. A higher magnification micrograph of the transition zone between the base and weld material is shown in Fig. 19. Similar to the AA5754 material, the melt appears to have begun abruptly with epitaxial growth of the base material into the weld. Additionally, a similar small cell size is noted in the weld.

4.2 Tensile Testing

Tensile testing was performed on the AA5182 alloy in an identical method as the earlier AA5754 and AA6111 twbs.

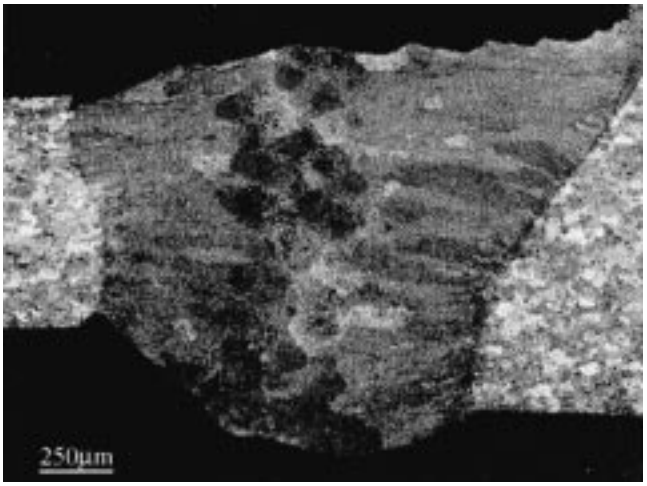

Fig. 22 Weld zone in the AA5182 twb after tensile deformation

Necking and subsequent failure of all the AA5182 samples occurred on the thin side of the twb away from the weld. A stress-strain curve for this test is shown in Fig. 20. While it appears that the elongation is approximately 13%, measurements of gauge lengths before and after testing show that there was only 1.5% strain on the thick side of the twb; hence, almost all of the deformation was contained on the thin side of the twb. Average strain to failure on the thin side of the twb was 24.4%, based on length measurements before and after deformation. This value of strain to failure is typical for this alloy.

To compare the tensile results from the twb to the as-received material, the strain data from the tests on the twb (Fig. 20) were recalculated to account for the strain isolating on the thin side of the blank. The gauge length was roughly approximated as half of the original gauge length to approximate the tensile coupon design and strain distribution. This is shown in Fig. 21 along with the as-received tensile curve for this alloy. The tensile characteristics of the twb, after recalculating, are very close to those of the as-received material. This indicates that the weld did not play a critical role in the tensile deformation of the blank, but rather the twb acted nearly as a tensile bar with a gauge length of only the thin part of the blank. The difference in strains to failure is most likely due to the rough approximation of gauge size in this recalculation.

As shown in the weld profiles before (Fig. 17) and after (Fig. 22) tensile deformation, the blank has a gradual weld profile that allows for the weld to resist strain localization. This can be seen in the relatively low β value of 0.59 for this twb (Table 3). In comparison, the weld profile of AA5754 (Fig. 2) has a somewhat reduced cross section at the top of the weld due to the fact that it was manufactured from two identical gauge sheets. That is, there is not enough molten material available in these blanks to form a weld without a reduction in cross-sectional area. This results in low resistance to strain localization in the weld during tensile deformation.

4.3 Formability Testing

Conventional limiting dome height (LDH) tests were performed on the AA5182 twb with the two different weld line

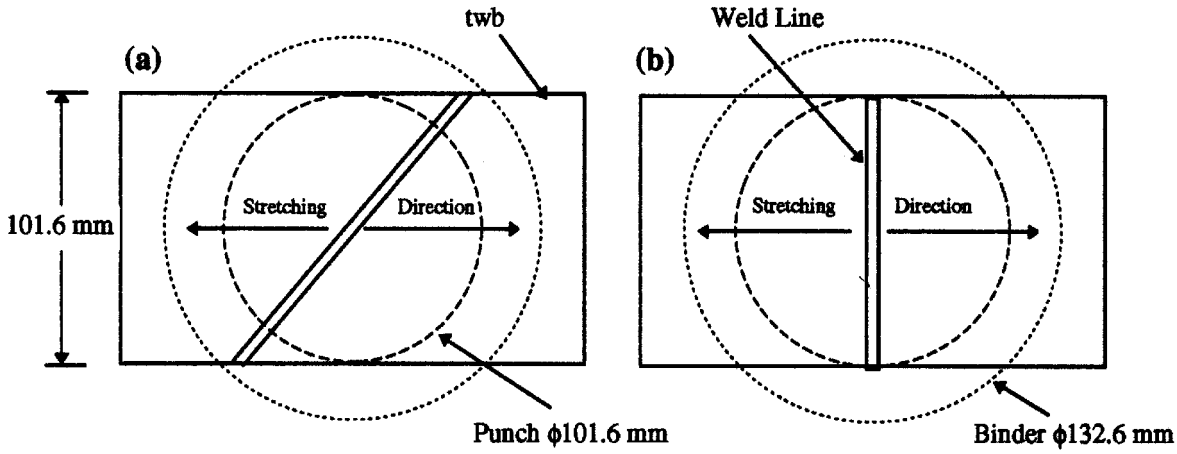

Fig. 23 Weld line orientation (**a**) at 45° and (**b**) at 90° to the stretching direction

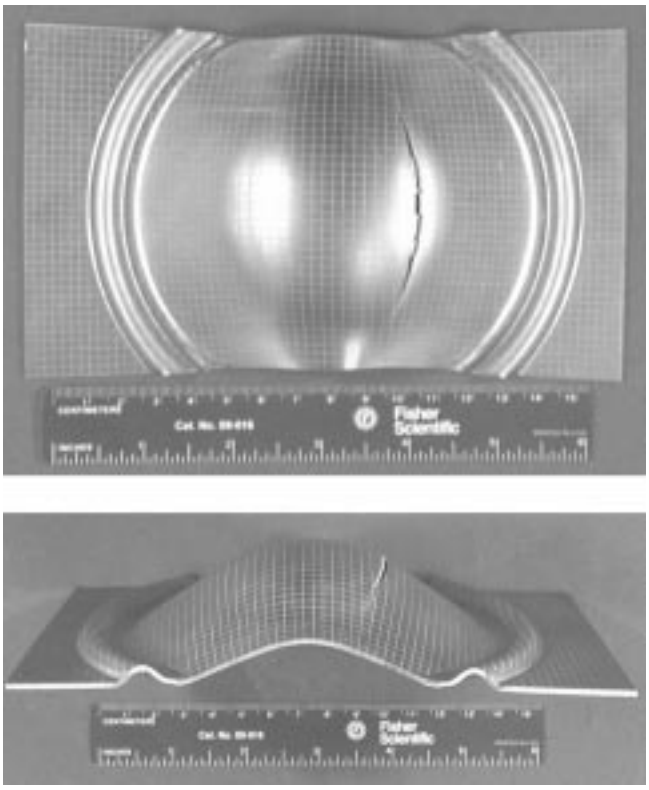

Fig. 24 Example of a formed AA5182 LDH specimen (no weld line)

Table 4 Summary of LDH test results on AA5182 twbs and unwelded blanks

Weld orientation (degrees)	Average punch penetration (mm)	Standard deviation of punch penetration (mm)
45	21.33	0.073
90	15.05	0.945
No weld	25.77	0.079

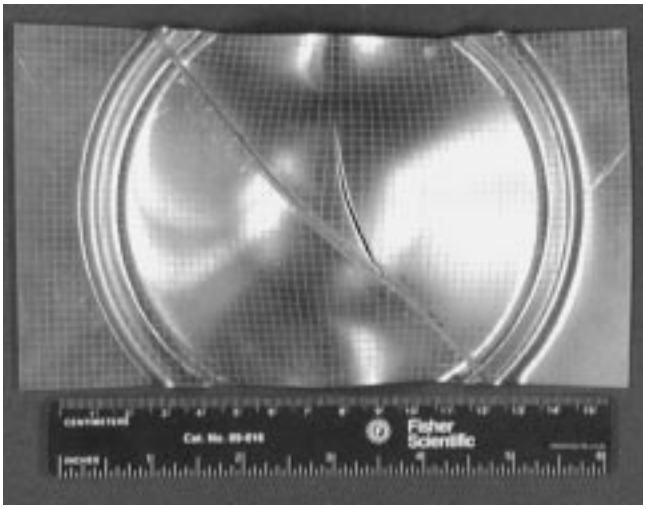

(**a**)

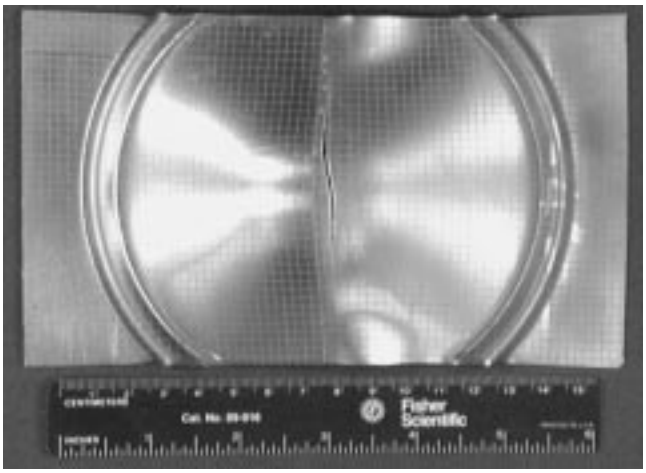

(**b**)

Fig. 25 The LDH samples after forming of the AA5182 blanks with the weld line oriented (**a**) 45° and (**b**) 90° to the major stretch direction

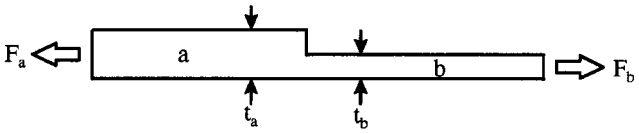

Fig. 26 Schematic of dissimilar gauge twb tensile deformation model

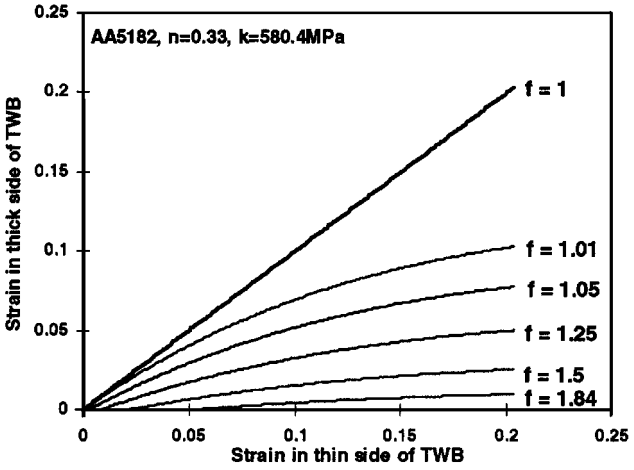

Fig. 27 Strain in the thick side of the weld plotted as a function of strain in the thin side of the weld for various values of *f* as determined from the tensile deformation model

orientations (45° to the stretching direction and 90° to the stretching direction) shown in Fig. 23 and compared with LDH tests on unwelded sheets. The test specimens (101.6 × 177.8 mm) were designed to produce a state of plane strain that represents both the condition with the lowest strains to failure and the strain state in which most automotive panels fail. Samples containing a weld were oriented so that the side opposite the welding surface made contact with the punch, as described earlier and shown in Fig. 17.

The LDH testing was performed on multiples of each specimen type using an MTS formability testing machine equipped with a 101.6 mm diameter hemispherical punch. The tests were conducted to fracture under dry conditions and at a constant punch speed of 5 mm/s. The LDH test results are shown in Table 4. The results show that twbs with weld orientations at 45° to the stretching direction have good formability compared with the base material. The formability drops substantially as the weld becomes perpendicular to the stretching direction.

None of the welded specimens failed in the weld, and all of them failed on the thin side of the twb. The specimens not containing a weld experienced typical failure with the crack initiation and propagation occurring in the unsupported section between the punch and the binder, as shown in Fig. 24. Failure in the specimens with the 45° weld orientation (Fig. 25a) experienced crack initiation near the weld. Once the crack reached the weld line, it propagated partially through the weld and continued to move parallel to the weld line. Failure in the specimens with 90° weld orientation (Fig. 25b) initiated within 5 mm of the edge of the weld and propagated parallel to the weld, but not through the weld. This can be attributed to the fact that the weld thickness at any point is larger than that of the thin sheet.

5. TWB Tensile Deformation Model

A tensile deformation model based on the twb sample shown in Fig. 26 has been constructed to investigate the effects of dissimilar gauge blanks. This simple model predicts the strain states in a twb of dissimilar gauges as it deforms in uniaxial tension. A schematic of this concept is shown in Fig. 26 and the mathematical formulation is detailed in the Appendix.

The strains in region a (thick side) are plotted as functions of strains in region b (thin side) in Fig. 27 for a number of *f* values (*f* = ratio of gauge in region a to gauge in region b). The 45° line represents a homogeneous straining situation where strain accumulates equally in regions a and b. With a 1% increase in gauge mismatch (*f* = 1.01), the strain attained in region a drops off significantly, to approximately half of the strain in region b at the end of the tensile test. With increasing *f* value, the strain that can be reached on the thick side of the twb decreases dramatically. For the *f* value of the AA5182 twb, *f* = 1.84 (*i.e.*, *f* = 1.55 mm/0.84 mm), the material on the thick side just begins to yield, accumulating approximately 1% strain before failure in region b. This is consistent with the experimental results where it was determined that the thick side of the blank reached a strain of approximately 1.5%.

6. Discussion

From the work on alloy consideration, it appears aluminum twbs have some distinct differences from the more conventional steel twbs. The steel twb, with its reduced gauge section (Fig. 8), is able to withstand tensile deformation because of the increased strength of the weld material. This is not the case in either of the two same-gauge aluminum twbs. To use aluminum twbs, engineers will have to design parts such that the weld line does not experience a large degree of stretching. This will become even more important in blanks where there is a substantial gauge differential.

Another potential loss of strength in the weld material for both alloys is from the increased size of the grains in the weld area. As shown in Fig. 3 and 4, the grain size in the weld material is significantly larger than the base material. According to the Hall-Petch relationship, this large disparity in grain size should result in a large difference in yield stress. However, a significant loss of strength in the weld was not detected in this alloy. It is believed that this predicted loss of strength is offset by the very small cell spacing produced from the rapid solidification. Therefore, it may be inferred that the solidification time during welding of these blanks is a major concern in terms of the resulting weld strength. The use of thicker gauge specimens may result in slower solidification times and therefore weaker welds.

To use twbs from AA6xxx series aluminum, it will be necessary to match the aging characteristics of the weld and base materials. One potential method of accomplishing this is to resolutionize the blank after welding. However, the associated

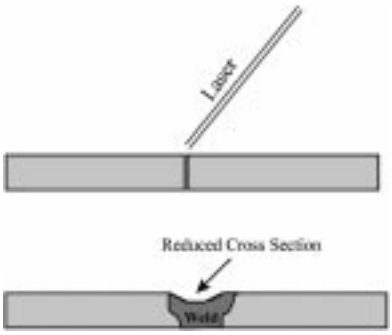

(**a**)

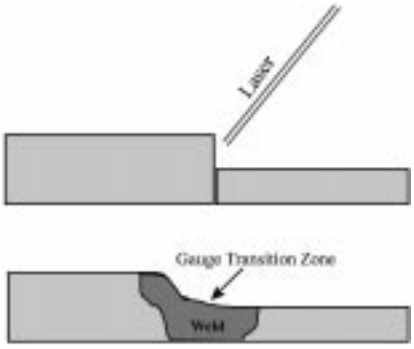

(**b**)

Fig. 28 Schematic of the welding of twbs of (**a**) same gauge and (**b**) different gauge blanks

cost penalty of this additional heat treatment may render using welded sheets from this alloy economically unfeasible. The potential of aluminum twbs in automotive structures is contingent upon their ability to withstand forming processes. The work on same-gauge AA5754 twbs proved that these blanks consistently fail in the weld during tensile deformation. However, the work on AA5182 twbs of dissimilar gauge has shown that these welds can resist tensile deformation and will probably be able to withstand many forming operations. As shown in Fig. 17, the gauge disparity in the AA5182 material results in a weld profile with a transition zone from one gauge to the other. In the same-gauge AA5754 twb, shown in Fig. 2, the blanks do not form this type of weld profile, but rather produce a slightly reduced cross-sectional area. This is due to the fact that the two blanks are of identical thickness and there is no material to form the transition zone.

Figure 28(a) is a schematic of two same-gauge blanks shown before and after welding. A reduced cross-sectional area is formed at the attachment point of the two blanks. This results from both the fact that when the blanks are welded material flows to fill the finite gap between the sheets and that some material is lost in welding. This is true in aluminum as well as steel twbs of identical gauge. In the case where there is a thickness differential, as shown in Fig. 28(b), the weld produces a transition zone between the two different gauge sheets. This welding is performed by melting the top part of the thicker material and allowing it to flow into the weld, thus forming the transition zone. This results in a dissimilar gauge twb with no reduction in cross-sectional area, thus allowing for higher load-carrying ability.

In the LDH testing of the welded blanks, the location of the crack initiation site near the weld is likely caused by the shape of the weld (Fig. 17). As discussed earlier, the weld line passes through the center of each specimen, and the punch contacts the specimen on the surface containing the bottom side of the weld. Visual inspection of the specimens showed that the protrusion in the bottom side of the weld resulted in delaying contact between the punch and the base material on both sides of the weld. This, in turn, left an unsupported section of the base material near the weld (the punch apex) that underwent high strains leading to fracture on the thin side of the twb. The thick side of the twb also experienced stretching, but due to the difference in thickness, higher levels of strain occurred in the thin side.

Although the effect of dissimilar gauges on strain distribution in twbs is more a function of geometry, the problem may be more severe in aluminum alloys because of their limited ductility. Premature failure in stamping may occur if the strain in the blank localizes on the thin part of a twb. Various methods have been attempted to limit strain inhomogeneities in twb forming, including varying the blank holder forces to preferentially allow material to flow into the die and designing dies to isolate the weld, thus allowing material to flow on both sides of the weld.

7. Summary and Conclusions

The switch from steel to aluminum twbs presents several technical challenges. Although engineers have been able to stamp steel twbs with relative ease because of the higher strength of the weld, it will not be as simple with aluminum twbs. Welding of aluminum blanks does not result in a similar increased strength in the weld and, therefore, will be more susceptible to failure in the weld during forming operations. The major issues with aluminum twbs in terms of the weld mechanics found in this study are summarized below.

- The elimination of the T4 temper in the 6111 material leaves the weld material significantly weaker than the base material. In this condition, this material would be nearly impossible to stamp and may be unreliable in service conditions. To equalize these strengths and create a useable welded sheet, it is necessary to resolutionize the blank prior to forming. Added costs associated with this extra heat treatment may render using this material economically unfeasible for twb applications.
- Tensile testing of twbs manufactured from same-gauge AA5754 sheet consistently failed in the weld. However, tensile tests on the dissimilar gauge AA5182 twb resulted in strain localization and failure outside of the weld area on the thin side of the weld for all samples tested. The reason for this difference in performance from the same-gauge AA5754 twb and the dissimilar AA5182 twb is believed to be a result of the melting of material in the thicker gauge material that creates a transition zone from one gauge to another.
- Material on the thin side of the dissimilar gauge AA5182 twb deformed to typical strains to failure for this alloy in tensile testing. Whereas the material work hardened on the thin side of the twb, material on the thick side reached

only a tensile strain of 1.5%. Results from the tensile deformation model demonstrated that even a slight mismatch in gauge can produce severe strain inhomogeneities between the two sides of a twb. For only a 1% difference in thickness, the strains were nearly double on the thin side of the twb at failure.

- The formability of AA5182-O twb depends strongly on the weld orientation. The formability drops as the weld orientation becomes perpendicular to the stretching direction, but good formability (about 80% of that of the base material) can be achieved with weld orientation at 45° to the stretching direction. Additionally, the shape of the weld impacts the failure location; in the investigated twb, the protrusion on the bottom side of the weld resulted in failure near the weld line.

Appendix

The model is based on a simple force balance between the two different gauges of the twb:

$$F_a = F_b \quad \text{(Eq A1)}$$

where F_a and F_b represent the tensile forces on the thick side, a, and thin side, b, of the twb, respectively. In terms of stress, this can be written as

$$\sigma_a = \frac{1}{f}\,\sigma_b \quad \text{(Eq A2)}$$

where σ_a and σ_b are the tensile stresses in regions a and b of the blank, respectively, and f is the ratio of cross-sectional areas (*i.e.*, $f = A_a/A_b$). With straining, f increases due to the preferential straining of the tensile bar on the thin side (region b). Based on the assumption of pure uniaxial stretching on both sides of the weld, f will increase as

$$f = f_0\, e^{\varepsilon_b - \varepsilon_a} \quad \text{(Eq A3)}$$

where f_0 is the initial thickness differential and ε_a and ε_b are the tensile strains in regions a and b, respectively. Assuming the material is rigid-plastic and follows a simple power-law hardening model, the stress in region b of the tensile bar is

$$\sigma_b = k\varepsilon_b^n \quad \text{(Eq A4)}$$

where k and n are material constants. Combining Eq A2 and A4, the stress in region a of the tensile bar is

$$\sigma_a = \frac{k}{f}\,\varepsilon_b^n \quad \text{(Eq A5)}$$

and the strain in region a is

$$\varepsilon_a = \left(\frac{\sigma_a}{k}\right)^{1/n} \quad \text{(Eq A6)}$$

The model algorithm begins by incrementing the strain in region b and then computing the cross-sectional mismatch, f, with Eq A3. The stress in region b is calculated with the simple work-hardening model in Eq A4, and the stress and strain in region a are then calculated with Eq A5 and A6. As the material on the thin side (region b) deforms and subsequently work hardens, the force F_b increases. With continued straining, the yield point on the thick side (region a) may be attained. Both sides of the material then continue to strain until the failure strain is reached on the thin side of the blank.

References

1. B. Irving: *Welding J.*, 1995, Aug., p. 49.
2. J.M. Trogolo and J.R. Dieffenbach: *Evaluation of Tailor Welded Blanks through Technical Cost Modeling*, SAE Report No. 980446, SAE, Warrendale, PA, 1998.
3. M.C. Stasik and R.H. Wagoner: *Aluminum and Magnesium for Automotive Applications*, Proc. TMS Conf., J.D. Bryant, ed., TMS, Warrendale, PA, 1996, p. 69.